Impact of Fracture Line Width on Radiographic Diagnosis of Vertical Root Fractures: Analysis of the Generalised Estimating Equation Model

Kaique LEITE DE LIMA[1], Lorena Rosa SILVA[1], Mozar ANDRADE MOTA NETO[2], Marcelo GUSMÃO PARAÍSO CAVALCANTI[3], Cláudio RODRIGUES LELES[1], Maria ALVES GARCIA SANTOS SILVA[1], Carlos ESTRELA[1], Brunno SANTOS DE FREITAS SILVA[1], Fernanda P YAMAMOTO-SILVA[1]

Objective: *To undertake a joint analysis of the influence of fracture width, dental thickness and distance of the fracture from the cortical bone on the radiographic diagnosis of vertical root fractures.*

Methods: *Thirty-six uniradicular bovine teeth were endodontically treated and distributed into three groups according to the remaining root dentine thickness: 1.2 mm, 1.5 mm and 1.8 mm. Each group comprised 12 teeth, six with vertical root fracture and six without. Scanning electron microscopy (SEM) images of the fractured tooth groups were obtained and the fracture lines were measured. All specimens were inserted into bone defects created in bovine ribs, at different distances from the external cortical bone. Digital periapical radiographs were randomly evaluated by three blinded examiners (presence or absence of fractures).*

Results: *The specificity for periapical radiography was found to be 89% and the accuracy rate was 57.4%. The mixed-model regression using the generalised estimating equation (GEE) model showed that the width of the fracture line and the thickness of the dental remnant play an important role in radiographic detection of vertical root fractures. There is a lower chance of correct diagnosis with fracture line widths < 0.2 mm (odds ratio [OR] 0.294, 95% confidence interval [CI] 0.103 to 0.836; P = 0.022) and tooth thicknesses < 1.2 mm (OR 0.342, 95% CI 0.157 to 0.747; P = 0.007).*

Conclusion: *Fracture line widths < 0.2 mm and smaller root thicknesses lead to a less accurate diagnosis of vertical root fractures on periapical radiographs.*

Key words: *diagnosis, endodontically treated teeth, radiograph, vertical root fracture*
Chin J Dent Res 2022;25(3):197–204; doi: 10.3290/j.cjdr.b3317977

Vertical root fracture (VRF) is characterised by a longitudinally orientated fracture plane that begins at the root apex and extends to the coronal part of the tooth[1]. Most signs and symptoms of VRF are nonspecific, thus limiting the reliability of the available methods for VRF detection[2]. CBCT has been suggested as a superior volumetric imaging system to periapical radiography in VRF diagnosis[3-6]; however, beam-hardening artefacts substantially reduce its performance[7] by hampering visualisation of or even mimicking the fracture line.

Incomplete root fractures are particularly difficult to detect on both periapical radiographs and CBCT[8]. Previous studies have compared periapical radiography and CBCT in assessing VRF[8-11] and revealed divergent and imprecise results for the two systems, thus hindering clear diagnosis of VRF and correct indication of the best system to use[1,12]. According to the American

1 Federal University of Goiás, Stomatological Sciences, Goiania, Brazil.
2 UniEVANGÉLICA University Centre of Anápolis, Anapolis, Brazil.
3 University of São Paulo, Sao Paulo, Brazil.

Corresponding author: Dr Brunno SANTOS DE FREITAS SILVA, Federal University of Goiás, Stomatological Sciences, Av. Primeira Avenida s/n, Goiania 74605-220, Brazil. Tel: 55-62-3209-6325. Email: brunno.santosfreitas@gmail.com

This study was funded in part by grants from the FUNADESP (#2020-21).

Academy of Oral and Maxillofacial Radiology, periapical radiography represents the initial imaging modality of choice in evaluating the suspected fractures[13] that may be observed on the root surface as a vertically orientated radiolucent line[8]. In fact, a fracture can only be visualised in radiographic examinations when the central beam of the x-rays is parallel to the fracture plane or within ± 4 degrees variation of it. Thus, a complementary approach recommends a horizontal angulation variation in radiographic images[15].

Several factors associated with image acquisition have been investigated for radiographic diagnosis of VRF, including the influence of root filling materials[16], the presence of metallic posts[9,17], comparison of different digital and conventional systems[18], the angulation in obtaining the radiographic images[15] and the influence of the fracture line width[3,4,10]. The results of these studies showed low accuracy of periapical radiography, especially because of the sensitivity of this examination method; however, these results should be interpreted with caution owing to the methodological differences across studies and the lack of simultaneous testing of the multiple predisposing factors that could influence the radiographic detection of VRF. For this reason, considering that periapical radiography is the main auxiliary method for diagnosing VRF and that current studies focus on individualised evaluation of the factors influencing its diagnosis, and are thus not very representative of clinical conditions, it is important to understand what dependent or joint factors are relevant to radiographic diagnosis of VRF. As such, this study aims to evaluate the influence of dental thickness, fracture width and the distance of fracture from the cortical bone in the radiographic diagnosis of VRF, using a methodology that considers the association of variables.

Materials and methods

This experimental study was approved by the Ethics Committee on Animal Research of our university (protocol no. 129/17).

Sample acquisition

Thirty-six single-rooted bovine teeth were acquired commercially from a specialist company (Mondelli Indústria de Alimentos, São Paulo, Brazil) for use as the study sample. The teeth were inspected microscopically (OPMI, Zeiss, Oberkochen, Germany) to examine the external root surfaces. Teeth exhibiting cracks, fractured cusps, pre-existing fractures (split tooth, complete or incomplete vertical root fracture), external resorptions, structural abnormalities or incomplete root formation were excluded.

Sample preparation

The crowns of the teeth were removed, leaving the remaining tooth at 15 mm in length. The samples were divided into three groups according to their visible dentine thickness: 1.2, 1.5 and 1.8 mm. These groups were based on the study by Katz and Tamse[19], who used a final mean thickness of 1.49 ± 0.16 mm after endodontic treatment. CBCT images (Orthopantomograph OP300, KaVo Dental, Tuusula, Finland) of the cervical, middle and apical regions were acquired and their thickness was measured using CS3D imaging software (v 3.1, Carestream Dental, Rochester, NY, USA). The final thickness of the dental remnant was established by taking the arithmetic mean of the three regions.

After random allocation of the groups, the sample units were worn using a #3 Peeso Reamer (Dentsply Maillefer, Ballaigues, Switzerland) in a motor at low rotation, guided by a digital caliper and periapical transoperative radiographs according to the group being studied. The root canals were then obturated using a thermoplastic technique with a McSpadden 0.50 condenser and gutta-percha cones (both Dentsply Maillefer) with epoxy amine resin cement (AH Plus, Dentsply Sirona, Charlotte, NC, USA).

Each group received 12 sample units, which were later divided randomly into six fractured and six non-fractured teeth. Simulation of the periodontal ligament for induction of VRF was performed according to the methodology proposed by Soares et al[20], after which fractures were induced using a universal test machine (Instron, TTDML, Canton, OH, USA) using a 2000 kg/force load cell at a speed of 0.05 mm/min.

Performing scanning electron microscopy (SEM)

SEM images of the fractured teeth were acquired to measure the fracture line (Figs 1 and 2). The teeth were dried at room temperature and scanned with a JEOL JSM IT300LV microscope (JEOL USA, Peabody, MA, USA) operating under a low vacuum, at a magnification of 15×. The image analysis was performed with ImageJ (National Institutes of Health, Bethesda, MD, USA), using the linear measurement tool in the cervical, middle and apical regions of the fracture tract. The final width was defined as the highest value found. The maximum fracture width in the sample ranged from 0.04 to 0.40 mm, with a mean of 0.14 ± 0.07 mm.

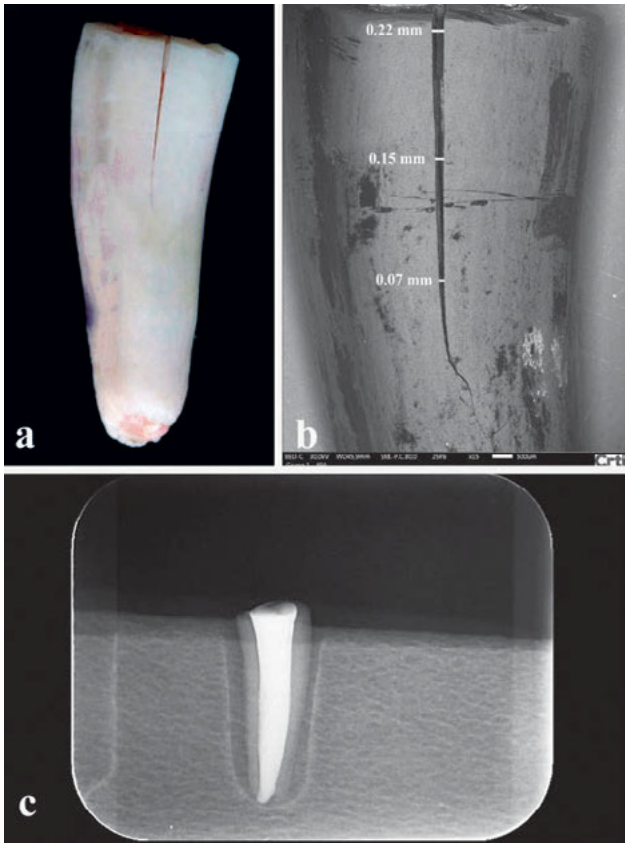

Fig 1 Dental remnant with fracture line < 0.2 mm. **(a)** Photograph of the fractured dental element. **(b)** SEM with 15× magnification, showing the fracture line. **(c)** Periapical radiograph with no evidence of VRF.

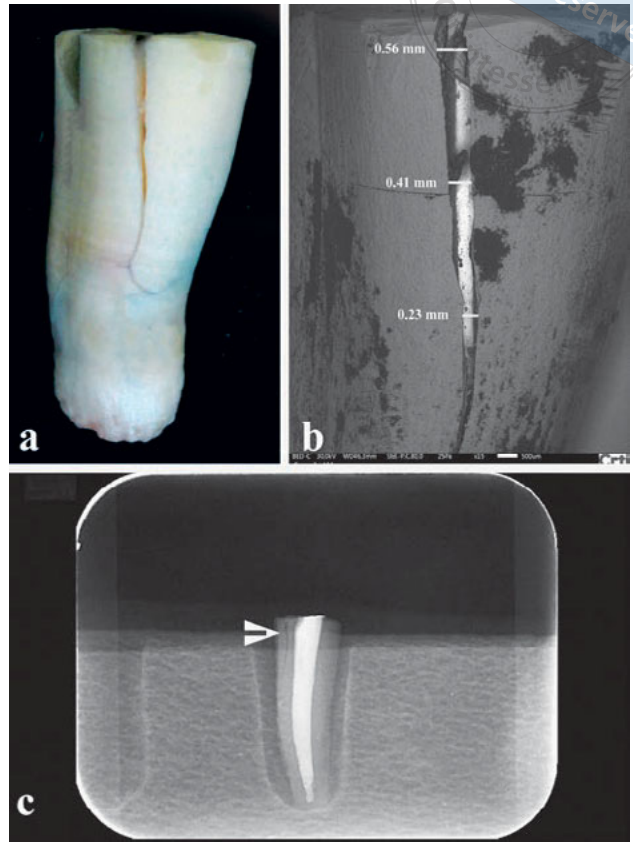

Fig 2 Dental remnant with fracture line > 0.2 mm. **(a)** Photograph of the fractured dental element. **(b)** SEM with 15× magnification, showing the fracture line. **(c)** Periapical radiograph with the radiolucent line on the proximal aspect compatible with VRF (arrowhead).

Phantom preparation

The cortical bone was simulated by using a bovine rib as a phantom. Bone defects were produced by simulating the dental alveoli (Fig 3). The phantom was prepared using a MaxiCut drill (American Burrs, Palhoça, Santa Catarina, Brazil) mounted on a low rotation motor to perform the scoring, which occurred at 1 mm on the cortical bone, and at a distance of 1 and 3 mm from the cortical bone.

Radiographic acquisition

Each tooth from each different group was radiographed individually in the three bovine rib bone defects being studied, which were surrounded by a thin layer of wax to simulate the attenuation of the x-ray beam. The images were acquired by positioning a phantom on an acrylic platform coupled to a transferor, as previously described by Nascimento et al[16].

All radiographic images were obtained using a Focus periapical unit (KaVo Dental) operating at 70 kVp and 7 mA and using size 2 phosphor plates (14.3 pl/mm, 886 × 1171 pixels) from the Express system (KaVo Dental). The exposure time was 0.2 s and a sensor-focus distance of 40 cm was used to obtain images at three horizontal angles, namely orthoradial, mesioradial and distoradial, with a variation of 15 degrees.

The images were analysed by simultaneously examining the three radiographs at different angulations of each tooth. Three calibrated and independent examiners, two radiologists and one endodontist, all with at least 5 years of experience, classified the images according to the evaluation presence of VRF using a 5-point scale: 1, VRF definitely present; 2, VRF probably present; 3, uncertain; 4, VRF probably absent; and 5, VRF definitely absent. All the images were evaluated in a low-light environment on an XPS X8700 computer with an Intel 3.4 GHz processor, 12 GB memory, 2 TB hard drive and a NVIDIA GeForce GTX 645 graphics

Fig 3 Bovine rib phantom used to evaluate the distance from the cortical bone. **(a)** 1 mm wear of cortical bone, **(b)** 1 mm from cortical bone and **(c)** 3 mm from cortical bone.

card (Dell, Austin, TX, USA) and a 28-inch colour monitor (UltraHD, Dell).

Data analysis

Data analysis was performed using SPSS software (version 24.0, IBM, Armonk, NY, USA). Descriptive statistics were used to summarise the data on VRF and independent factors. The VRF data classified by the raters were cross-tabulated with the dichotomous condition of the dental roots (whether fractured or not) to calculate the rates of the correct measures to be used in the overall measures, and by each of the raters, whose performance in the detection of VRF was expressed as accurate.

The outcome variable was labelled as a correct rating – code = 1 (true positive [TP] and true negative [TN] cases) or as an incorrect rating – code = 0 (false positive [FP] and false negative [FN] cases). Since the measurements were clustered among the raters and along the different distances of the cortical bone, there was a violation of the assumption of independence of data. Thus, correct identification of the root condition (fractured or not) was modelled by mixed-model regression using a generalised estimating equation (GEE).

The original database was changed to a format that rearranged the groups of related columns into groups of rows in the new data file using the "restructure" command in the software. The analysis was specified as a binomial distribution, and the Logit as the link function, in order to run the GEE model for the binary outcome. The independent factors in the regression model were the raters (three levels), the distance from the cortical bone (proximal, central and distal positions), the width of the fracture line (no fracture, < 0.2 mm and ≥ 0.2 mm) and the width of the remaining root structure (three levels). All the predictors were entered into the regression model using the forced entry method to test the main effects of each variable. GEE regression parameters were expressed as the odds ratio (OR) at a 95% confidence interval (CI). The significance of the model effects was tested using Wald chi-square statistics, and the statistical significance was set at $P < 0.05$.

Results

The sensitivity and specificity values, positive predictive value, negative predictive value and accuracy values for each examiner, in relation to the fracture diagnosed by periapical radiography, are presented in Table 1. The highest value found was for specificity, resulting in a greater ability to diagnose non-fractured teeth correctly according to 85% of all three evaluators. Periapical radiography presented a correct VRF detection rate of 57%.

Use of the GEE made it possible to establish that there was no statistically significant relation between the different evaluators or the distance of the cortical bone and the correct diagnosis of VRF (Table 2), considering $P < 0.05$ for all the variables. The width of the fracture line and the thickness of the dental remnant played an important role in detecting VRF, and the chance of correct diagnosis was lower when the fracture width was reduced (< 0.2 mm: OR 0.294, 95% CI 0.103 to 0.836; $P = 0.022$) or the remaining tooth was reduced (lower: OR 0.342, 95% CI 0.157 to 0.74; $P = 0.007$), except in non-fractured cases (OR 12.052, 95% CI 5.923 to 24.526; $P > 0.001$), which presented a greater chance of success than cases with width ≥ 0.2 mm.

Poor agreement was observed between the examiners in detecting VRF. Table 3 shows the interobserver kappa coefficients for VRF detection in periapical radiographs for each examiner. The intraexaminer kappa calculation indicated that substantial agreement was obtained in VRF detection, except for Examiner 1 (Table 4).

Discussion

In the present in vitro model, the width of the fracture line and the thickness of the dental remnant played important roles in VRF detection regardless of the distance from the tooth to the cortical bone. Fracture width seems to be a more determining factor for detection than dental remnant thickness, since larger fracture widths are more easily detected when the fracture plane is parallel to the central x-ray beam[14]. When the remaining tooth was reduced in dentine thickness, there was a smaller chance of correct VRF. This is because greater force was required to produce VRF in thicker teeth with the universal test machine, resulting in fractures with larger widths that favour their detection.

Table 1 Measurements taken from a 2 × 2 table applied to determine accuracy of assessment of teeth with possible VRF using periapical radiographs.

Rater	Number of images	Sensitivity	Specificity	Positive predictive value	Negative predictive value	Accuracy (%)
#1	108	0.51	0.61	0.57	0.55	0.56
#2	108	0.12	1.00	1.00	0.53	0.56
#3	108	0.22	0.96	0.85	0.55	0.59
Overall	324	0.29	0.85	0.67	0.54	0.57

Table 2 GEE parameters for the probability of correct diagnosis of VRF in radiographs.

Parameter		OR	95% CI		Significance
			Lower	Upper	
Intercept		1.301	0.473	3.581	0.610
Rater	#1	0.828	0.269	2.551	0.742
	#2	0.828	0.555	1.235	0.354
	#3	1.000	0.000	0.000	0.000
Distance to cortical bone	Proximal	0.647	0.355	1.177	0.154
	Central	1.066	0.586	1.939	0.834
	Distal	1.000	0.000	0.000	0.000
Width of fracture line	No fracture	12.052	5.923	24.526	> 0.001
	< 0.2 mm	0.294	0.103	0.836	0.022
	≥ 0.2 mm	1.000	0.000	0.000	0.000
Chance of correct diagnosis with remaining root structure width	Lower	0.342	0.157	0.747	0.007
	Intermediary	0.464	0.167	1.284	0.139
	Higher	1.000	0.000	0.000	0.000

Table 3 Kappa values for interexaminer agreement in interpreting periapical radiographs for VRF diagnosis.

	K value
Examiner 1 × Examiner 2	0.036
Examiner 1 × Examiner 3	0.072
Examiner 2 × Examiner 3	0.531

Table 4 Kappa values for intraexaminer agreement of VRF diagnosis.

	K value
Examiner 1	0.293
Examiner 2	0.730
Examiner 3	0.738

Several studies have investigated the accuracy of periapical radiographs in detecting an artificially made VRF and reported similar results, with low sensitivity and high specificity values[9-11]. Our main objective was not to confirm the difficulty of VRF radiographic detection, but rather to understand the impact of factors acting simultaneously to influence the formation/definition of the radiographic image in VRF diagnosis using a regression model.

The present authors formed three experimental groups composed of teeth with different thicknesses. The selection considered the influence of dentine thickness in the development of VRF[21] and the knowledge that VRF is more prevalent in teeth with a reduced dental structure, such as mandibular molars and maxillary premolars[22-24], often with endodontic treatment[25] and/or with intraradicular retainers[26,27]. The remaining tooth thickness may vary according to the type of teeth, the endodontic instrumentation technique (manual, rotary, etc.)[25,28] and the type of preparation made to receive an intraradicular retainer[29]. In this respect, reduced dental structure is associated with greater susceptibility to VRF[30] and greater radiographic sharpness. A smaller thickness offers less resistance to x-ray attenuation and may thus favour greater radiographic sharpness, facilitating radiographic detection of VRF[31]. Despite the greater sharpness of the radiographic image of the dental thickness, this did not facilitate correct diagnosis of VRF in the present study.

We also hypothesised that the distance from the tooth to the cortical bone would influence the radiographic detection of VRF. This could be an important factor to study since the different dental groups have distinctive positions in relation to the bone, e.g., anterior teeth are usually implanted closer to the cortical bone compared to the posterior teeth[32]. This hypothesis can be explained by the fact that superimposition of a thicker bone layer can make it difficult to visualise

radiolucent structures in radiographic images[33] since objects located along the long axis of an x-ray beam are projected to the same spot on the radiographic receptor. Thus, the proximity of fractured teeth to the cortical bone and the image receptor may increase the sharpness of the images, which could facilitate VRF diagnosis; however, the present data show that the distance of the cortical bone from the VRF was not a factor associated with VRF detection.

Our model also included an analysis of fracture width. Brady et al[10] compared the accuracy of periapical radiography and CBCT in detecting both complete (when fragments are separated) and incomplete VRF (when fragments are not separated) in endodontically untreated teeth in an ex vivo model. Comparison of complete versus incomplete VRF revealed that the area under the receiver operating characteristic curve was not significant, but that the sensitivity was significantly higher in the group with complete fracture than that with incomplete fracture. In our study, the accuracy of periapical radiography was low, corroborating previous studies[8,10,11]; however, our model of analysis did not separate the teeth into complete or incomplete fracture groups, because it was believed that fracture width does not necessarily imply that fragments are separated, but does influence their detection. The fracture width must be great enough for the x-ray beam to cross it in order to form a radiographic image[12]. Separated fragments would indeed aid in the diagnosis of VRF by revealing other radiographic signs, such as periradicular bone loss[34].

Patel et al[8] used a methodology similar to that of Brady et al[10] to create fractures in endodontically treated human teeth. They reported that no incomplete fracture (0.05 to 0.11 mm) was detected radiographically, and that only 19% of complete fractures (> 0.2 mm) were detected[8]. They also stated that both radiographically and CBCT-generated area under the curve values are inaccurate[8]. Özer[3] compared the ability of both CBCT and digital periapical radiography to diagnose VRF of different thicknesses (< 0.2 mm, 0.2 mm and 0.4 mm) and concluded that radiographs presented better results, concurrently with larger fracture thicknesses; moreover, 41.6% of the fractures < 0.2 mm were correctly diagnosed, and 60% of all the fractures were 0.4 mm thick. Corroborating their findings, we found that fractures > 0.2 mm were more likely to be diagnosed compared with fractures < 0.2 mm, regardless of the distance between the dental structure and the cortical bone or the thickness of the tooth.

This in vitro model with bovine teeth allowed the impact of cortical distance, tooth thickness and fracture width to be evaluated jointly and controllably in performing VRF diagnosis. Despite the limitations inherent to an in vitro study, use of the bovine model allowed standardisation of the tooth length, shape and age, thus reducing the bias related to these parameters. The chemical composition and tensile strength and modulus of elasticity of bovine tooth enamel and dentine are mostly similar to those of human teeth, making bovine alternatives the first choice when replacing human teeth for research purposes[35-37]. Despite the morphological differences between bovine and human teeth, studies with bovine teeth have presented results comparable to those obtained with extracted human teeth[35].

This study used high resolution SEM images to determine the fracture line width accurately, thus allowing microstructural visualisation and high image magnification[23], which enabled assigned limits to be evaluated clearly. The quantitative analysis from SEM images is a feasible technique conventionally performed with the ImageJ image processing tool[38].

Since periapical radiography is the first auxiliary method to evaluate a suspected fracture, it is important to understand its limitations in order to be more rational and specific in indicating the most suitable imaging option. The present results corroborate those of Özer[3] and Patel et al[8] and show that when the VRF cannot be identified radiographically, this is probably due to its small width. In this case, CBCT with a voxel size < 0.2 mm is indicated and increases the chance of VRF detection, even in the presence of artefacts.

Conclusion

In conclusion, diagnosis of VRF using digital periapical radiographs is influenced by the width of the fracture line. A distance > 0.2 mm between dental fragments tends to provide a greater number of correct diagnoses of VRF.

Conflicts of interest

The authors declare no conflicts of interest related to this study.

Author contribution

Drs Kaique LEITE DE LIMA, Lorena Rosa SILVA, Cláudio RODRIGUES LELES and Brunno SANTOS DE FREITAS SILVA contributed to the data analysis; Drs Kaique LEITE DE LIMA and Lorena Rosa SILVA contributed to the data gathering. All authors contributed to the writing and editing of the manuscript.

(Received Oct 20, 2021, accepted Apr 02, 2022)

References

1. Chang E, Lam E, Shah P, Azarpazhooh A. Cone-beam computed tomography for detecting vertical root fractures in endodontically treated teeth: A systematic review. J Endod 2016;42:177–185.
2. Patel S, Brown J, Pimentel T, Kelly RD, Abella F, Durack C. Cone beam computed tomography in Endodontics – A review of the literature. Int Endod J 2019;52:1138–1152.
3. Ozer SY. Detection of vertical root fractures of different thicknesses in endodontically enlarged teeth by cone beam computed tomography versus digital radiography. J Endod 2010;36:1245–1249.
4. Makeeva IM, Byakova SF, Novozhilova NE, et al. Detection of artificially induced vertical root fractures of different widths by cone beam computed tomography in vitro and in vivo. Int Endod J 2016;49: 980–989.
5. Khedmat S, Rouhi N, Drage N, Shokouhinejad N, Nekoofar MH. Evaluation of three imaging techniques for the detection of vertical root fractures in the absence and presence of gutta-percha root fillings. Int Endod J 2012;45:1004–1009.
6. Avsever H, Gunduz K, Orhan K, et al. Comparison of intraoral radiography and cone-beam computed tomography for the detection of horizontal root fractures: An in vitro study. Clin Oral Investig 2014;18:285–292.
7. Talwar S, Utneja S, Nawal RR, Kaushik A, Srivastava D, Oberoy SS. Role of cone-beam computed tomography in diagnosis of vertical root fractures: A systematic review and meta-analysis. J Endod 2016;42:12–24.
8. Patel S, Brady E, Wilson R, Brown J, Mannocci F. The detection of vertical root fractures in root filled teeth with periapical radiographs and CBCT scans. Int Endod J 2013;46:1140–1152.
9. Junqueira RB, Verner FS, Campos CN, Devito KL, do Carmo AM. Detection of vertical root fractures in the presence of intracanal metallic post: A comparison between periapical radiography and cone-beam computed tomography. J Endod 2013;39:1620–1624.
10. Brady E, Mannocci F, Brown J, Wilson R, Patel S. A comparison of cone beam computed tomography and periapical radiography for the detection of vertical root fractures in nonendodontically treated teeth. Int Endod J 2014;47:735–746.
11. Chavda R, Mannocci F, Andiappan M, Patel S. Comparing the in vivo diagnostic accuracy of digital periapical radiography with cone-beam computed tomography for the detection of vertical root fracture. J Endod 2014;40:1524–1529.
12. Tsesis I, Rosen E, Tamse A, Taschieri S, Kfir A. Diagnosis of vertical root fractures in endodontically treated teeth based on clinical and radiographic indices: A systematic review. J Endod 2010;36: 1455–1458.
13. Special Committee to Revise the Joint AAE/AAOMR Position Statement on use of CBCT in Endodontics. AAE and AAOMR joint position statement: Use of Cone Beam Computed Tomography in Endodontics 2015 Update. Oral Surg Oral Med Oral Pathol Oral Radiol 2015;120:508–512.
14. Pitts DL, Natkin E. Diagnosis and treatment of vertical root fractures. J Endod 1983;9:338–346.
15. Wenzel A, Kirkevang LL. High resolution charge-coupled device sensor vs. medium resolution photostimulable phosphor plate digital receptors for detection of root fractures in vitro. Dent Traumatol 2005;21:32–36.
16. Nascimento HA, Neves FS, de-Azevedo-Vaz SL, Duque TM, Ambrosano GM, Freitas DQ. Impact of root fillings and posts on the diagnostic ability of three intra-oral digital radiographic systems in detecting vertical root fractures. Int Endod J 2015;48:864–871.
17. Jakobson SJ, Westphalen VP, Silva Neto UX, Fariniuk LF, Schroeder AG, Carneiro E. The influence of metallic posts in the detection of vertical root fractures using different imaging examinations. Dentomaxillofac Radiol 2014;43:20130287.
18. Tofangchiha M, Bakhshi M, Fakhar HB, Panjnoush M. Conventional and digital radiography in vertical root fracture diagnosis: A comparison study. Dent Traumatol 2011;27:143–146.
19. Katz A, Tamse A. A combined radiographic and computerized scanning method to evaluate remaining dentine thickness in mandibular incisors after various intracanal procedures. Int Endod J 2003;36: 682–686.
20. Soares CJ, Pizi EC, Fonseca RB, Martins LR. Influence of root embedment material and periodontal ligament simulation on fracture resistance tests. Braz Oral Res 2005;19:11–16.
21. Silva LR, de Lima KL, Santos AA, et al. Dentin thickness as a risk factor for vertical root fracture in endodontically treated teeth: A case-control study. Clin Oral Investig 2021;25:1099–1105.
22. Cohen S, Berman LH, Blanco L, Bakland L, Kim JS. A demographic analysis of vertical root fractures. J Endod 2006;32:1160–1163.
23. PradeepKumar AR, Shemesh H, Jothilatha S, Vijayabharathi R, Jayalakshmi S, Kishen A. Diagnosis of vertical root fractures in restored endodontically treated teeth: A time-dependent retrospective cohort study. J Endod 2016;42:1175–1180.
24. Liao WC, Tsai YL, Wang CY, et al. Clinical and radiographic characteristics of vertical root fractures in endodontically and nonendodontically treated teeth. J Endod 2017;43:687–693.
25. Tang W, Wu Y, Smales RJ. Identifying and reducing risks for potential fractures in endodontically treated teeth. J Endod 2010;36:609–617.
26. Marchi GM, Mitsui FH, Cavalcanti AN. Effect of remaining dentine structure and thermal-mechanical aging on the fracture resistance of bovine roots with different post and core systems. Int Endod J 2008;41:969–976.
27. Junqueira RB, de Carvalho RF, Marinho CC, Valera MC, Carvalho CAT. Influence of glass fibre post length and remaining dentine thickness on the fracture resistance of root filled teeth. Int Endod J 2017;50:569–577.
28. Singla M, Aggarwal V, Logani A, Shah N. Comparative evaluation of rotary ProTaper, Profile, and conventional stepback technique on reduction in Enterococcus faecalis colony-forming units and vertical root fracture resistance of root canals. Oral Surg Oral Med Oral Pathol Oral Radiol Endod 2010;109:e105–e110.
29. Souza EM, do Nascimento LM, Maia Filho EM, Alves CM. The impact of post preparation on the residual dentin thickness of maxillary molars. J Prosthet Dent 2011;106:184–190.
30. Mireku AS, Romberg E, Fouad AF, Arola D. Vertical fracture of root filled teeth restored with posts: the effects of patient age and dentine thickness. Int Endod J 2010;43:218–225.
31. Patel S, Dawood A, Whaites E, Pitt Ford T. New dimensions in endodontic imaging: Part 1. Conventional and alternative radiographic systems. Int Endod J 2009;42:447–462.
32. Ohiomoba H, Sonis A, Yansane A, Friedland B. Quantitative evaluation of maxillary alveolar cortical bone thickness and density using computed tomography imaging. Am J Orthod Dentofacial Orthop 2017;151:82–91.
33. Bender IB, Seltzer S. Roentgenographic and direct observation of experimental lesions in bone: II. 1961. J Endod 2003;29:707–712; discussion 701.
34. Tamse A. Vertical root fractures in endodontically treated teeth: Diagnostic signs and clinical management. Endodontic Topics 2006;13:84–94.
35. Soares FZ, Follak A, da Rosa LS, Montagner AF, Lenzi TL, Rocha RO. Bovine tooth is a substitute for human tooth on bond strength studies: A systematic review and meta-analysis of in vitro studies. Dent Mater 2016;32:1385–1393.
36. Sano H, Ciucchi B, Matthews WG, Pashley DH. Tensile properties of mineralized and demineralized human and bovine dentin. J Dent Res 1994;73:1205–1211.

37. Teruel Jde D, Alcolea A, Hernández A, Ruiz AJ. Comparison of chemical composition of enamel and dentine in human, bovine, porcine and ovine teeth. Arch Oral Biol 2015;60:768–775.

38. Schneider CA, Rasband WS, Eliceiri KW. NIH Image to ImageJ: 25 years of image analysis. Nat Methods 2012;9:671–675.